Identification of Dynamic Stiffness of Squeeze Film Damper using Active Magnetic Bearing System as an Exciter

KIM, K.-J. and LEE, C.-W.
Center for Noise and Vibration Control (NOVIC), Dept. of Mechanical Eng., KAIST, Science Town, Daejeon, KOREA

ABSTRACT

The dynamic characteristics of an oil-lubricated, short squeeze film damper (SFD) with a central feeding groove are derived based on a theoretical analysis considering the effect of the groove, and identified experimentally using an Active Magnetic Bearing (AMB) system as an exciter. In order to get the theoretical solution, the fluid film forces of the grooved SFD are analytically derived so that the dynamic coefficients of the SFD are expressed in terms of its design parameters. For the experimental validation of the applied analysis, a test rig using an AMB as an exciter is proposed. Using this test rig, a number of experiments are extensively conducted with different values of clearance in order to investigate its effect on the dynamic characteristics and the performance of the SFD. Damping and inertia coefficients of the SFD experimentally identified are compared with the analytical results to demonstrate the effectiveness of the analysis. It is also shown that the AMB is an ideal device for tests of SFDs.

Keywords: squeeze film damper, dynamic characteristics, active magnetic bearing, central feeding groove

1. INTRODUCTION

Due to its relatively simple structure and high damping characteristics, a SFD is known as a suitable mechanical element for the damping device of high-speed rotating machinery supported by the rolling element bearings and, therefore, has been adopted for a common aircraft engine since it was invented. In general, a SFD is said to be a bearing system that accommodates the mechanical advantages of journal bearings and ball bearings, and its structure is the combination of these typical bearing systems: the rotor is supported by a ball bearing and rotates with the inner raceway of the ball bearing, but the outer raceway (the journal of a SFD) of the rolling element only whirls, without rotating motion, in the housing of a SFD. This vibratory motion of the journal will squeeze the lubricants which are filled at the clearance region between the outer raceway and housing. The squeeze action results in the development of pressure field within fluid film, and the resultant force works as a damping mechanism for the vibration of a SFD [1,2]. Though much research effort have been expanded to establish the predictive and theoretical expressions of a SFD, but most of those analyses available in the open literature are not completely satisfactory because, in spite of the development of sophisticated theories, there are still some discrepancies between analyses and experiments. Therefore, many research groups have attempted to obtain the dynamic characteristics of a SFD experimentally [3-5].

In this paper, the dynamic characteristics of a grooved short SFD with an open-ended boundary condition are identified theoretically and experimentally. In order to identify the dynamic coefficients of a short SFD experimentally, the SFD is designed and fabricated, and the testing system using an AMB as an exciter is proposed. In addition, theoretical analysis considering the effect of a central feeding groove is applied to derive the dynamic

characteristics of a SFD and to evaluate the experimental results. Extensive experiments are carried out to investigate the effect of the clearance change on the dynamic properties and performance of SFDs.

2. MOTIVATION OF RESEARCH

One of the most well-known test methods used to identify the dynamic characteristics of fluid film bearings, i.e. journal bearings, is the excitation of a bearing by means of a specially designed complex test rig [6]. However, the necessity of an additional complex apparatus is pointed out as one of the crucial disadvantage of those methods. To overcome the disadvantage of a conventional test rig, an AMB is used as an exciter for the testing system.

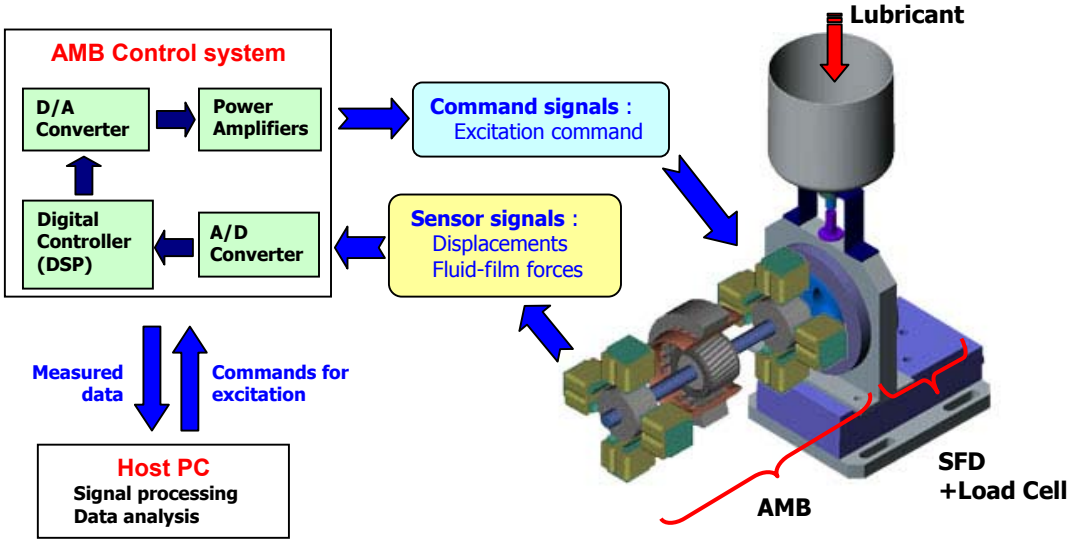

Figure 1. Scheme of the experimental setup

In Figure 1, the schematic diagram of the proposed experimental setup and the input/output relationship of data are described: the shaft of an AMB, which is connected with the journal of a SFD, is supported by two individual magnetic bearings and, the housing of a SFD is placed at the end of the AMB to assemble the entire test rig with ease. The test rig is installed on the rigid structure and, therefore, isolated from the vibration coming from ground. In addition, most experiments are conducted within 0-50*Hz* frequency ranges since the first elastic mode of the shaft exists above 200*Hz*.

By means of the control algorithm of an AMB system, a user can easily manipulate the amplitude and the frequency of an excitation command. Fluid film forces generated by the excitation of a journal can be measured by a 3-axis tool dynamometer installed under the housing of a SFD. This housing-attached measurement has an advantage that it can measure pure fluid film forces. The displacements of a journal and the fluid film forces can be analyzed after saving into a PC equipped with a digital signal processing (DSP) board. The described setup allows a number of possibilities that are new for rotordynamic experiments, including:

- arbitrary selection of the static operating position of a journal within the allowed clearance range of an AMB
- contact-free excitation
- arbitrary manipulation of excitation amplitudes, phases and frequency
- generation of various situations which might happen at a rotor-bearing system

The cross-sectional view of the SFD designed for this work is shown in Figure 2. Using different journal diameters, the clearance of the SFD can be changed. In addition, the specifications of the AMB system are listed in Table 1. Among the listed specifications, the capability as an exciter can be inferred from the value of the AMB's radial air gap.

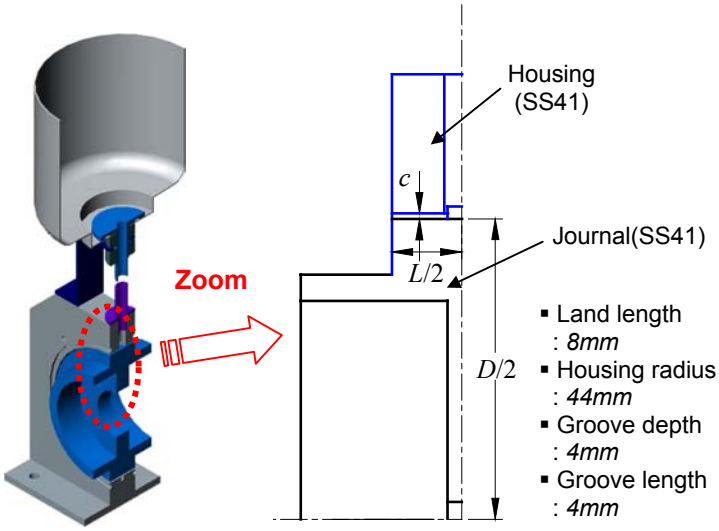

Figure 2. Cross-sectional view of the designed SFD

Electro-magnet and Rotor	
Radial air gap/Rotor diameter	g_a=0.88mm / ϕ=89mm
Magnetic coils	N=400 turns, L_o=56mH
Rotor mass	m=8.34kg
Peripheral electronic devices	
Sensor & Amplifier	Eddy current type, Resolution: 0.5μm Gain: K_s=5V/mm, Bandwidth: 20kHz

Table 1. Specifications of the AMB system [7]

3. DERIVATION OF DYNAMIC CHARACTERISTICS

For the theoretical solution, the dynamic coefficients of a grooved SFD are analytically derived. Consider the laminar flow in the thin film lands of a short open ends damper with a central feeding groove as shown in Figure 3. In this structure, the lubricant is delivered to the large volume groove through feeding devices, and then, flows axially to the damper ends. The flow is confined to the narrow annular region between a stationary housing and an inner, nonrotating journal. The journal motion is assumed to be small amplitude oscillation (e<<c) of frequency ω about the bearing center. The applied coordinate systems are also shown in Figure 3. The principal assumptions introduced for this analysis are the following:

- the fluid on the film lands is incompressible and isoviscous
- the axial length of a journal is small compared to its circumferential extent (short bearing assumption)
- at the central groove, the fluid is regarded as slightly compressible and acts as a dynamic compliance because of its large volume
- no slip conditions can be used at the journal/housing surface

The bulk flow equations describing the fluid flow within the film lands of a SFD are given in dimensionless form as [8]:

$$\frac{\partial}{\partial x}(hu)+\frac{\partial h}{\partial \tau}=0 \tag{1}$$

$$-h\frac{\partial p}{\partial x}=12\frac{u}{h}+\gamma \mathrm{Re}_s\frac{\partial}{\partial \tau}(hu) \tag{2}$$

In the equations above, $\mathrm{Re}_s=\rho\omega c^2/\mu$ is the squeeze film Reynolds number. The inertial velocity

parameter γ is equal to 1.2 for small Reynolds number ($Re_s \rightarrow 0$), and approaches a value of 1.0 for inviscid flow conditions ($Re_s \rightarrow \infty$).

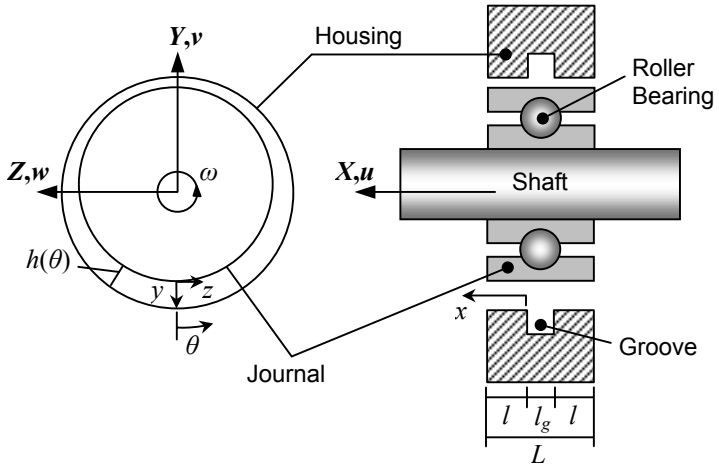

Figure 3. Geometry of a SFD with a central feeding groove

For small amplitude motions about the bearing center, the dynamic film thickness can be described by the real part of,

$$h = 1 + \left(\varepsilon_Y \cos\theta + \varepsilon_Z \sin\theta\right) e^{j\tau} = 1 + \varepsilon_m h_m e^{j\tau} \tag{3}$$

In this equation, $\varepsilon_Y, \varepsilon_Z << 1$, $m=Y$ or Z, $\tau=\omega t$, $h_Y=\cos\theta$, and $h_Z=\sin\theta$. Referred to *Mulcahy* [9], the dynamic pressure and axial bulk flow velocity field can be expressed in a similar way as:

$$p = p_m \varepsilon_m e^{j\tau}, \quad u = u_m \varepsilon_m e^{j\tau} \tag{4}$$

The boundary conditions for the dynamic pressure field are,

$$p = p_{ambient} = 0 \quad \text{at} \quad x = x_o = l/R \tag{5a}$$

$$p = p_e(\theta,\tau) = p_{me}(\theta)\varepsilon_m e^{j\tau} \quad \text{at} \quad x = 0 \tag{5b}$$

where p_e represents the dynamic pressure at the location where the groove meets the squeeze film land. This pressure can be obtained from a mass flow balance at the groove volume.

Substituting the variables defined in Eqs.(3) and (4) into Eqs.(1) and (2) and neglecting higher order terms (ε_Y^2, $\varepsilon_Z^2 << 1$) simplify the bulk flow equations as ordinary differential equations.

$$\frac{du_m}{dx} + jh_m = 0 \tag{6}$$

$$\frac{dp_m}{dx} = -\left(12 + j\gamma \,\mathrm{Re}_s\right) u_m \tag{7}$$

The expression for the axial velocity field and pressure field can be obtained by integrating these equations as:

$$u_m = u_{me} - jxh_m \tag{8}$$

$$p_m = p_{me} - \left(12 + j\gamma \,\mathrm{Re}_s\right)\left(u_{me}x - jh_m x^2/2\right) \tag{9}$$

where u_{me} indicates the inlet axial velocity at the location of the groove-squeeze film land interface. Substitution of the boundary conditions specified in Eqs.(5) into the dynamic pressure field expression yields

$$p_m = -\left(12 + j\gamma \,\mathrm{Re}_s\right) jh_m \frac{x}{2}\left(x_o - x\right) + p_{me}\left(1 - \frac{x}{x_o}\right) \tag{10}$$

and the axial velocity u_{me} at the entrance and the dynamic groove pressure p_{me} have the relationship defined as following.

$$u_{me} = a_u p_{me} + jb_u h_m \tag{11}$$

where $a_u=1/x_o(12+j\gamma \mathrm{Re}_s)$, $b_u=x_o/2$.

According to the conventional analyses, the dynamic pressure at the central feeding groove is considered to be null, i.e., $p_{me}=0$, and thus, the pressure distribution is determined based on this oversimplified assumption. However, experimental evidence shows that the pressure at this region is not null [10,11]. Therefore, in order to get the reasonable modeling for a grooved SFD, it is crucial to consider the effect of a groove.

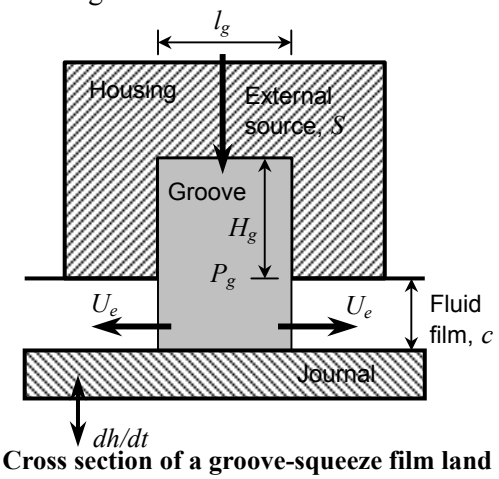

Figure 4. Cross section of a groove-squeeze film land [8]

In this work, a capacitance model with liquid compressibility is applied for the consideration of the groove effect. Due to the mass continuity interaction in the large volume groove region, the dynamic pressure field is generated at the groove-squeeze film land interface. Consider a cross section of the groove-squeeze film land as described in Figure 4. Then, a differential mass flow balance equation can be expressed as [8]:

$$S(z)-\Delta m_z=\Delta m_x+\frac{\partial}{\partial t}\left(\rho \Delta U_g\right) \tag{12}$$

where, $\Delta U_g=(H_g+H)l_g\Delta z$ represents the groove differential volume and $\Delta m_x=2\rho H U_e \Delta z$ represents the differential axial flow into the film lands. Δm_z and $S(z)$ are the groove circumferential flow and the term accounting for local feeding/discharge sources (e.g. orifices, slots, etc), respectively. As assumed in the beginning of this analysis, the liquid in the groove is slightly compressible and it can be expressed as $d\rho=\rho\beta dp$. In this expression, β means a compressibility factor. As Δz goes to zero, Eq.(12) can be rewritten in dimensionless form as:

$$s(\theta)-\frac{\partial \overline{m}_z}{\partial \theta}=2hu_e+\frac{l_g}{R}\frac{\partial h}{\partial \tau}+\lambda\frac{\partial p_e}{\partial \tau} \tag{13}$$

where, λ $(=\mu\omega\beta(l_gR/c^2)(H_g+c)/c)$ indicates the groove frequency-liquid compressibility parameter. This parameter is proportional to the excitation frequency ω, the ratio of groove depth to film clearance, and the compressibility factor β.

As mentioned earlier, according to the short bearing assumption, the circumferential flow variation can be considered as negligible. Furthermore, for simplicity of the analysis, the source term accounting for the local feeding/discharge of the damper is assumed to have minimal local dynamic effect. Then, the flow balance equation at the groove interface can be reduced to the following one.

$$0=2u_{me}+j\left(\frac{l_g}{R}h_m+\lambda p_{me}\right) \tag{14}$$

Combination of Eqs.(11) and (14) yields the dynamic groove pressure as:

$$p_{me}=-j\frac{2b_u+l_g/R}{2a_u+j\lambda}h_m=-j\frac{\left(L+l_g\right)\left(L-l_g\right)}{2D^2}\frac{\left(12+j\gamma \mathrm{Re}_s\right)}{\left(1-\kappa_r\right)+j\kappa_i}h_m \triangleq -j\Delta p_e h_m \tag{15}$$

where,

$$\kappa_r = \gamma\rho\omega^2\beta\frac{l_g\left(L-l_g\right)}{4}\left(h_g+1\right),\quad \kappa_i = 3\mu\omega\beta\frac{l_g\left(L-l_g\right)}{c^2}\left(h_g+1\right) \tag{16}$$

Note that the dynamic groove pressure p_{me} is obtained as constant value within the entire groove width l_g. This simplification is valid for grooves having small damper length to groove width ratios (l_g/L<<1). Moreover, in most applications, groove widths do not exceed *20 percent* of the total damper length.

Finally, the dynamic pressure field given in Eq.(10) can be expressed as:

$$p_m = -jh_m\left\{\left(12+j\gamma\,\mathrm{Re}_s\right)\frac{x}{2}\left(x_o-x\right)+\Delta p_e\left(1-\frac{x}{x_o}\right)\right\} \tag{17}$$

In Eq.(17), the first term represents the well known pressure field equation for an open ends short SFD using conventional theory; while the second term shows the groove volume-liquid compressibility effect on the squeeze film land pressure. Figure 5 shows the pressure field distributions within the SFD and, especially, in the axial direction at $\theta=\pi$. Due to the groove effect, the entire pressure distribution, as shown in Figure 5, has larger level in comparison with the result using the conventional analysis.

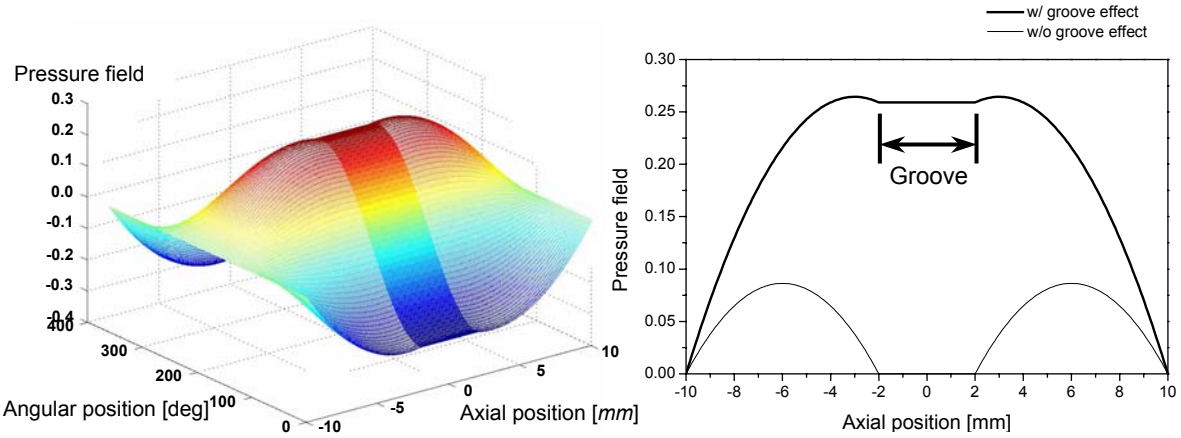

(a) 3-dimensional distribution **(b) axial distribution where $\theta=\pi$**

Figure 5. Pressure field at a grooved SFD

Fluid film force coefficients can be obtained by integrating the dynamic pressure field over the entire journal surface, i.e.,

$$K_{mn}-\omega^2M_{mn}+j\omega C_{mn} = -\frac{2\mu\omega R^4}{c^3}\int_0^{2\pi}\left\{\int_0^{\frac{l_g}{D}}p_{me}dx+\int_0^{x_o}p_m dx\right\}h_n d\theta \tag{18}$$

where subscript mn (m, n=Y, Z) means the m-directional component of the fluid film forces generated by the journal motion in n-direction. Some straightforward algebraic substitutions give the dynamic properties of fluid film forces given by:

$$K_{YY}=K_{ZZ}=K_{YZ}=K_{ZY}=0 \tag{19a}$$

$$C_{YY}=C_{ZZ}=C_o\left(1+\frac{\sigma}{\Pi}\right),\quad C_{YZ}=C_{ZY}=0 \tag{19b}$$

$$M_{YY}=M_{ZZ}=M_o\gamma\left[1+\frac{\sigma}{\Pi}\left\{\left(1-\kappa_r\right)-\frac{\kappa_i^2}{\kappa_r}\right\}\right],\quad M_{YZ}=M_{ZY}=0 \tag{19c}$$

where,

$$\Pi=\left(1-\kappa_r\right)^2+\kappa_i^2,\quad \sigma=3\frac{\left(L+l_g\right)^2}{\left(L-l_g\right)^2}$$

$$C_o = \frac{\pi}{4}\mu R\frac{\left(L-l_g\right)^3}{c^3},\quad M_o = \frac{\pi}{48}\rho\frac{R}{c}\left(L-l_g\right)^3 \tag{20}$$

4. EXPERIMENTAL IDENTIFICATION METHOD

When the test rig excites the journal of a SFD, the generated fluid film forces are measured by a 3-axis tool dynamometer in horizontal and vertical directions at the same time, respectively. Each of the fluid film forces can be determined by the displacement, velocity and acceleration of the journal under excitation. Therefore, the fluid film forces can be expressed in matrix form given by:

$$\begin{Bmatrix} F_Y \\ F_Z \end{Bmatrix} = \begin{bmatrix} K_{YY} & K_{YZ} \\ K_{ZY} & K_{ZZ} \end{bmatrix}\begin{Bmatrix} Y \\ Z \end{Bmatrix} + \begin{bmatrix} C_{YY} & C_{YZ} \\ C_{ZY} & C_{ZZ} \end{bmatrix}\begin{Bmatrix} \dot{Y} \\ \dot{Z} \end{Bmatrix} + \begin{bmatrix} M_{YY} & M_{YZ} \\ M_{ZY} & M_{ZZ} \end{bmatrix}\begin{Bmatrix} \ddot{Y} \\ \ddot{Z} \end{Bmatrix} \tag{21}$$

For the harmonic excitation with an arbitrary excitation frequency ω, Eq.(21) can be rewritten as

$$\begin{aligned} \begin{Bmatrix} F_Y(j\omega) \\ F_Z(j\omega) \end{Bmatrix} &= \begin{bmatrix} K_{YY}-\omega^2 M_{YY}+j\omega C_{YY} & K_{YZ}-\omega^2 M_{YZ}+j\omega C_{YZ} \\ K_{ZY}-\omega^2 M_{ZY}+j\omega C_{ZY} & K_{ZZ}-\omega^2 M_{ZZ}+j\omega C_{ZZ} \end{bmatrix}\begin{Bmatrix} Y(\omega) \\ Z(\omega) \end{Bmatrix} \\ &= \begin{bmatrix} D_{YY}(j\omega) & D_{YZ}(j\omega) \\ D_{ZY}(j\omega) & D_{ZZ}(j\omega) \end{bmatrix}\begin{Bmatrix} Y(\omega) \\ Z(\omega) \end{Bmatrix} \end{aligned} \tag{22}$$

The dynamic coefficients of a SFD can be obtained experimentally by separating the real and imaginary part from the measured dynamic stiffness $D_{mn}(j\omega)$ (m, n=Y, Z). To obtain the entire four elements of the dynamic stiffness matrix (DSM), the excitation must be carried out in Y- and Z-directions independently, and the vertical and the horizontal fluid film forces should be measured for each case.

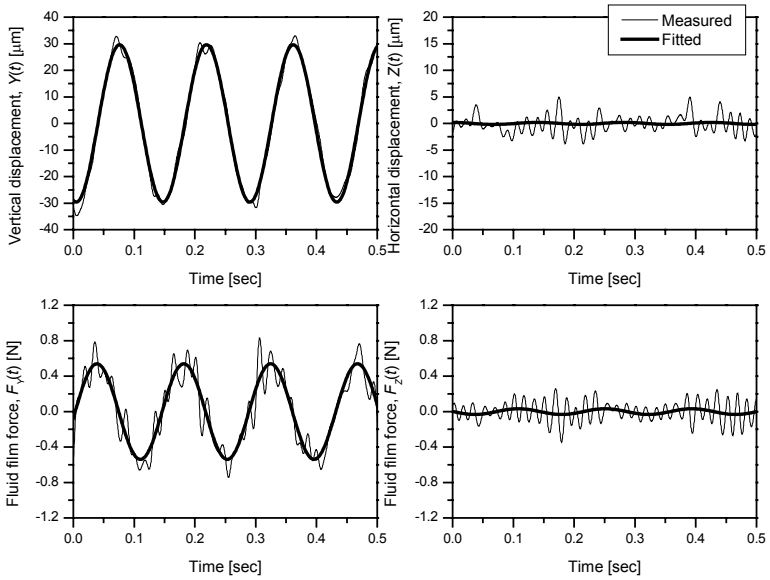

Figure 6. Measured signals vs. fitted results using the least square error method : 7Hz, zero static center position, and vertical excitation

In order to quantify the magnitude of the measured forces and displacements of a journal, the acquired signals can be approximated as a pure-tone harmonic signal using the least square error method in time domain. This method has advantages that no spectral leakage occurs and no triggering/windowing is necessary, and that it is also valid for very noisy signals [12]. For example, a measured vertical displacement signal $Y(t)$ can be approximated as a pure harmonic function $Y'(t)$ as follow:

$$Y(t) \approx Y'(t) = A_Y \sin(\omega t + \varphi) = A_Y \cos\varphi \cdot \sin\omega t + A_Y \sin\varphi \cdot \cos\omega t \tag{23}$$

In Eq.(23), the excitation frequency ω is already a known value and, therefore, the unknowns are an amplitude A_Y and a phase φ. To determine these unknown parameters, the least square error method can be applied to the measured signal as

$$\begin{bmatrix} \sin\omega t \cdot \sin\omega t & \cos\omega t \cdot \sin\omega t \\ \sin\omega t \cdot \cos\omega t & \cos\omega t \cdot \cos\omega t \end{bmatrix} \begin{Bmatrix} A_Y \cos\varphi \\ A_Y \sin\varphi \end{Bmatrix} = \begin{Bmatrix} Y(t) \cdot \sin\omega t \\ Y(t) \cdot \cos\omega t \end{Bmatrix} \tag{24}$$

In Figure 6, the approximated results in a least squares sense are plotted with the measured displacements and fluid film forces when the journal is excited in vertical direction with 7*Hz* frequency and *zero* static center position. The results show that the approximated results fit well with the measured data. However, the measured data in unexcited direction are corrupted with the noisy signals of sensors, but their order of the magnitude is less than 10% compared with that of main components.

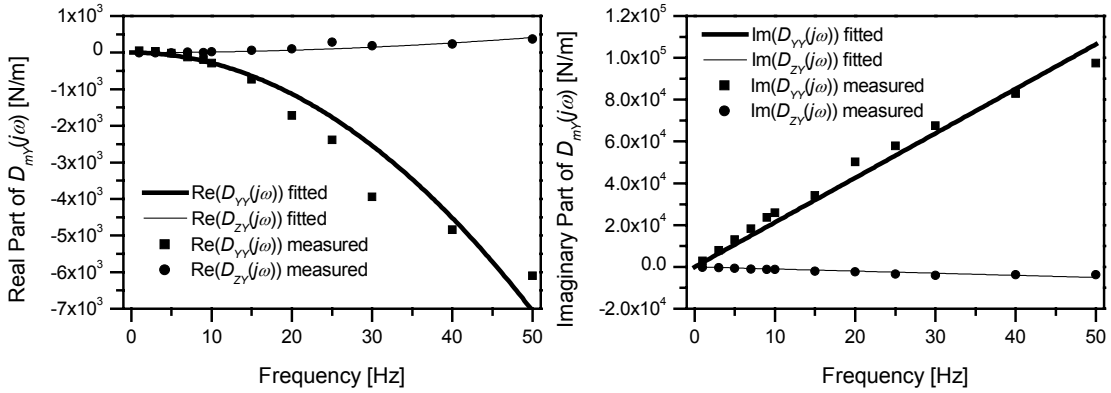

Figure 7. Measured dynamic characteristics

The analyzed results using the explained identification method are shown in Figure 7. The experimental results plotted in Figure 7 are obtained by measuring the fluid film forces F_Y and F_Z under the excitation in vertical direction. In this experiment, the radial clearance is 0.8*mm* and the viscosity of lubricant is 0.046*Pa-sec*. The open-ended design is used for the boundary condition of the SFD.

Results in Figure 7 show that the fluid film forces generated in the short open-ended SFD mainly consist of the damping and inertia effect. The real part of dynamic stiffness shows that the stiffness effect is negligibly small and the inertia effect coming from the acceleration of fluid is dominant. According to the published papers [1], this inertia effect becomes dominant when the viscosity of the lubricant is low and the frequency of an excitation is high. However, the imaginary part shows that the damping force is dominant, and the damping coefficient is nearly independent of the frequency change.

5. EXPERIMENTAL RESULTS

Until now, most research efforts for SFDs have been focused on the identification of nonlinearities coming from the large journal eccentricity. However, the investigation about the influence of design parameters is not studied sufficiently. In general, the performance of SFDs is influenced by some important design parameters, e.g., radial clearance, land length and seal width. There are more design parameters such as the viscosity of lubricant and the supply pressure, but their effect is relatively small. However, the influence of those important design parameters needs to be investigated to verify their contribution to the dynamic characteristics and to design a SFD effectively.

The influence of the radial clearance is investigated and the experimental results are shown in Figure 8. In these results, the design set of radial clearances is 0.4*mm*, 0.6*mm*, and 0.8*mm*. The

lubricant having 0.046*Pa-sec* as its viscosity is used and the boundary conditions are open-end. In Figure 8, the magnitude of the damping and inertia coefficients decrease as the clearance increases, and the cross-coupled terms in the DSM are small compared with the diagonal terms. These results mean that the fluid film force perpendicular to the direction of a journal movement does not exist in SFDs since the journal does not rotate.

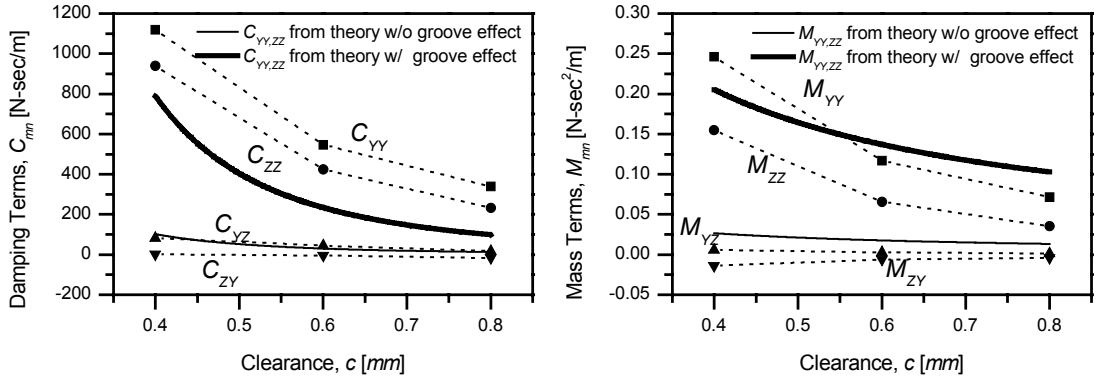

Figure 8. Measured vs. predicted dynamic characteristics: clearance effect (symbols: measured data, lines: predicted data)

This figure also includes the theoretical predictions from the improved model and conventional one together. Over the tested frequency range, the results from the grooved-SFD model correlate very well with the test data, and thus, show the accuracy of the analysis considering the groove effect. However, the conventional model underestimates the experimental results on the order of one-eighth. Therefore, these results mean that the consideration of the groove effect in the analysis is vital.

6. CONCLUSION

In this work, the excitation system using an AMB system as an exciter is proposed and the dynamic characteristics of an oil-lubricated, short SFD with a central feeding groove are identified in theoretical and experimental approaches. The analytical solutions for the fluid film forces of a grooved-SFD are derived and the corresponding dynamic coefficients are obtained theoretically. The governing equation for the fluid film forces is transformed to the frequency domain and the dynamic stiffness matrix is identified. In order to identify the dynamic characteristics experimentally, the grooved-SFD with open ends is designed and its prototype is made. Using this SFD and the proposed test rig, the fluid film forces are measured and analyzed. Extensive experiments are conducted to evaluate the influence of the radial clearance and these results are compared with the analytical solutions. Compared data show that the predicted dynamic properties, which is obtained from the analysis considering the effect of a central feeding groove, correlate well with the test results. These results prove that the consideration of the groove effect is important in a SFD modeling and enable the effective design of system to provide appropriate dynamic characteristics to a rotor-bearing system. In addition, the ability of an AMB as an exciter for the testing of fluid film bearings is also proved.

7. REFERENCES

1. Zeidan, F.Y., San Andres, L. and Vance, J.M., Design and application of squeeze film dampers in rotating machinery, *Proceedings of the twenty-fifth turbomachinery symposium*, (1996) 169-188.
2. Zeidan, F.Y., Application of squeeze film dampers, *Turbomachinery International*, (1995) 50-53.
3. Burrows, C.R. and Sahinkaya, Frequency-domain estimation of linearized oil-film

coefficients, *ASME Journal of Lubrication Technology*, Vol. 104 (1982) 210-215.
4. Zhang, J., Roberts, J.B. and Ellis, J., Experimental behavior of a short cylindrical squeeze film damper executing circular centered orbits, *ASME Journal of Tribology*, Vol. 115 (1994) 528-534.
5. Knopf, E. and Nordmann, R., Identification of the dynamic characteristics of turbulent journal bearings using active magnetic bearings, *International conference on Vibrations in Rotating Machinery*, Nottingham (2000) 381-390.
6. Someya, T., *Journal-bearing databook*, Springer-Verlag (1988).
7. Kim, C.-S. and Lee, C.-W., Isotropic optimal control of active magnetic bearing system, *ASME Journal of Dynamic Systems, Measurement, and Control*, Vol. 118, No. 4 (1996) 721-726.
8. San Andres, L., Analysis of short squeeze film dampers with a central groove, *ASME Journal of Tribology*, Vol. 114 (1992) 659-665.
9. Mulcahy, T.M., Fluid forces on rods vibrating in finite length annular regions, *ASME Journal of Applied Mechanics*, Vol. 47 (1980) 234-240.
10. Arauz, G.L. and San Andres, L., Effect of a circumferential feeding groove on the dynamic force response of a short squeeze film damper, *ASME Journal of Tribology*, Vol. 116 (1994) 369-377.
11. Arauz, G.L. and San Andres, L., Experimental study on the effect of a circumferential feeding groove on the dynamic force response of a sealed squeeze film damper, *ASME Journal of Tribology*, Vol. 118 (1996) 900-905.
12. Hoffman, J.D., *Numerical methods for engineers and scientists*, McGraw-Hill (1992).

7. NOMENCLATURE

c	radial clearance
C_{mn}	damping coefficients
D	journal diameter
D_{mn}	dynamic stiffness
e_m	journal displacement
h	dimensionless film thickness
H_g	groove depth, $h_g=H_g/c$
K_{mn}	stiffness coefficients
l, l_g, L	land length, groove length, total damper length, respectively
m_x	ρUH, axial mass flow rate per unit circumferential length
M_{mn}	inertia force coefficients
p	$P/(\mu\omega R^2/c^2)$, dimensionless pressure
R	journal radius, $R=D/2$
u	$U/\omega R$, dimensionless mean flow axial velocity
x_o	$l/R=(L-l_g)/D$, dimensionless land length
x, y, z	rotational coordinates
X, Y, Z	inertial coordinate system
ε_m	journal eccentricity, $\varepsilon_m=e_m/c$
θ	z/R, circumferential coordinates
μ	viscosity of lubricant
ρ	density of lubricant
τ	ωt, dimensionless time
ω	excitation frequency

Subscripts

$(\cdot)_e$	at the groove-squeeze film land interface
$(\cdot)_{m,n}$	Y- or/and Z-directional component